Stress transfer in the Lazufre volcanic area, central Andes

J. Ruch,[1,2] A. Manconi,[1,3] G. Zeni,[3] G. Solaro,[3,4] A. Pepe,[3] M. Shirzaei,[1] T. R. Walter,[1] and R. Lanari[3]

Received 6 October 2009; accepted 12 October 2009; published 21 November 2009.

[1] We generated a 13-year InSAR time series from 1995–2008 to investigate the spatiotemporal characteristics of two neighboring volcano's deformations for the Lazufre volcanic area, central Andes. The data reveal two scales of uplift initiating during the observation time: (1) a large-scale uplift started in 1997 that shows an increase of the mean uplift rate of up to 3.2 cm/yr, now affecting several eruptive centers situated in an area larger than 1800 km^2 and (2) a small-scale uplift located at Lastarria volcano, which is the only volcano to show strong fumarolic activity in decades, with most of the clear deformation apparently not observed before 2000. Both the large and small uplift signals can be explained by magmatic or hydrothermal sources located at about 13 km and 1 km deep, respectively. To test a possible relationship, we use numerical modeling and estimate that the depth inflating source increased the tensile stress close to the shallow source. We discuss how the deep inflating source may have disturbed the shallow one and triggered the observed deformation at Lastarria.
Citation: Ruch, J., A. Manconi, G. Zeni, G. Solaro, A. Pepe, M. Shirzaei, T. R. Walter, and R. Lanari (2009), Stress transfer in the Lazufre volcanic area, central Andes, *Geophys. Res. Lett.*, *36*, L22303, doi:10.1029/2009GL041276.

1. Introduction

[2] Stress field changes in volcanic areas have often been hypothesized to be responsible for sudden, unexpected eruptions at volcanoes that are close to a critical state [*Hill et al.*, 2002]. However, the importance of stress changes associated with adjacent volcanoes is poorly documented, and responsible processes are not well understood. Here we investigate two overlapping deformation signals affecting the Lazufre volcanic area and the Lastarria volcano, and stress field change model suggest a possible relationship.

[3] The Lazufre volcanic area (central Andes) is located on the Chilean-Argentinean border about 300 km east of the subduction trench (Figure 1a). It is part of the highly elevated Altiplano Puna Plateau that started to form during the Eocene period, resulting from the convergence of the Nazca and the South American plates [*Oncken et al.*, 2006, and references therein]. The area contains several morphologically distinct volcanic centers [*De Silva and Francis*, 1991]. Only one of these, the Lastarria volcano (~5700 m asl), shows strong and persistent fumarolic activity localized on the recent crater borders and on the western flank (Figure 1f). No historic eruptions have been reported [*Naranjo and Francis*, 1987].

[4] Through InSAR (interferometric synthetic aperture radar) studies, a large-scale elliptical deformation signal was detected during the period from 1998 to 2000 with a deformation rate of about 1 cm/yr [*Pritchard and Simons*, 2002]. At that time, the inflation dimension reached about 35 km across the long axis [*Pritchard and Simons*, 2004] and then increased up to 50 km [*Froger et al.*, 2007; *Ruch et al.*, 2008]. Source depth estimates are between 9 and 17 km, probably related to magma intrusion [*Pritchard and Simons*, 2004]. In addition, a second inflation signal, occurring at a smaller scale and affecting the Lastarria volcano was revealed. A very shallow pressurized source located at ~1 km beneath the surface was used to explain the Lastarria deformation for the period from 2003 to 2005 [*Froger et al.*, 2007]. Nevertheless, the timing of these inflating volcanic systems as well as their relationship have not yet been evaluated.

[5] Here we investigate the temporal relationship between the two revealed deformation signals by carrying out an advanced analysis on InSAR data spanning from 1995 to 2008. In addition, through numerical modeling, we suggest that the stress change caused by the inflation of the deep source probably triggered the activity observed at Lastarria by increasing the tensile stress in the surroundings of the shallow source.

2. Deformation Measurements

[6] Two SAR datasets acquired by the European Satellite missions ERS-1/2 and ENVISAT, operating in descending orbits were used in this study (track 282, frame 4118). The ERS dataset includes 21 images spanning the period from June 1995 to December 2006, while the 24 ENVISAT acquisitions span from March 2003 to January 2008. Both datasets have the same illumination geometry (~23° look angle). The phase difference (interferogram) between temporally separated SAR image pairs has been exploited via InSAR techniques [*Massonnet and Feigl*, 1998] to get an estimate of the ground deformation projection in the radar sensor's line-of-sight (LOS). We computed a total of 153 interferograms characterized by spatial baseline values smaller than 500 m. To retrieve the mean deformation velocity maps of the area and the corresponding displacement time series, we applied the SBAS algorithm [*Berardino et al.*, 2002], which also allows the filtering of possible atmospheric artifacts (see auxiliary material).[5]

[1]Deutsches GeoForschungsZentrum, Potsdam, Germany.
[2]Dipartimento di Scienze Geologiche, Roma Tre, Rome, Italy.
[3]IREA, CNR, Naples, Italy.
[4]Osservatorio Vesuviano, Istituto Nazionale di Geofisica e Vulcanologia, Naples, Italy.

0094-8276/09/2009GL041276$05.00

[5]Auxiliary materials are available in the HTML. doi:10.1029/2009GL041276.

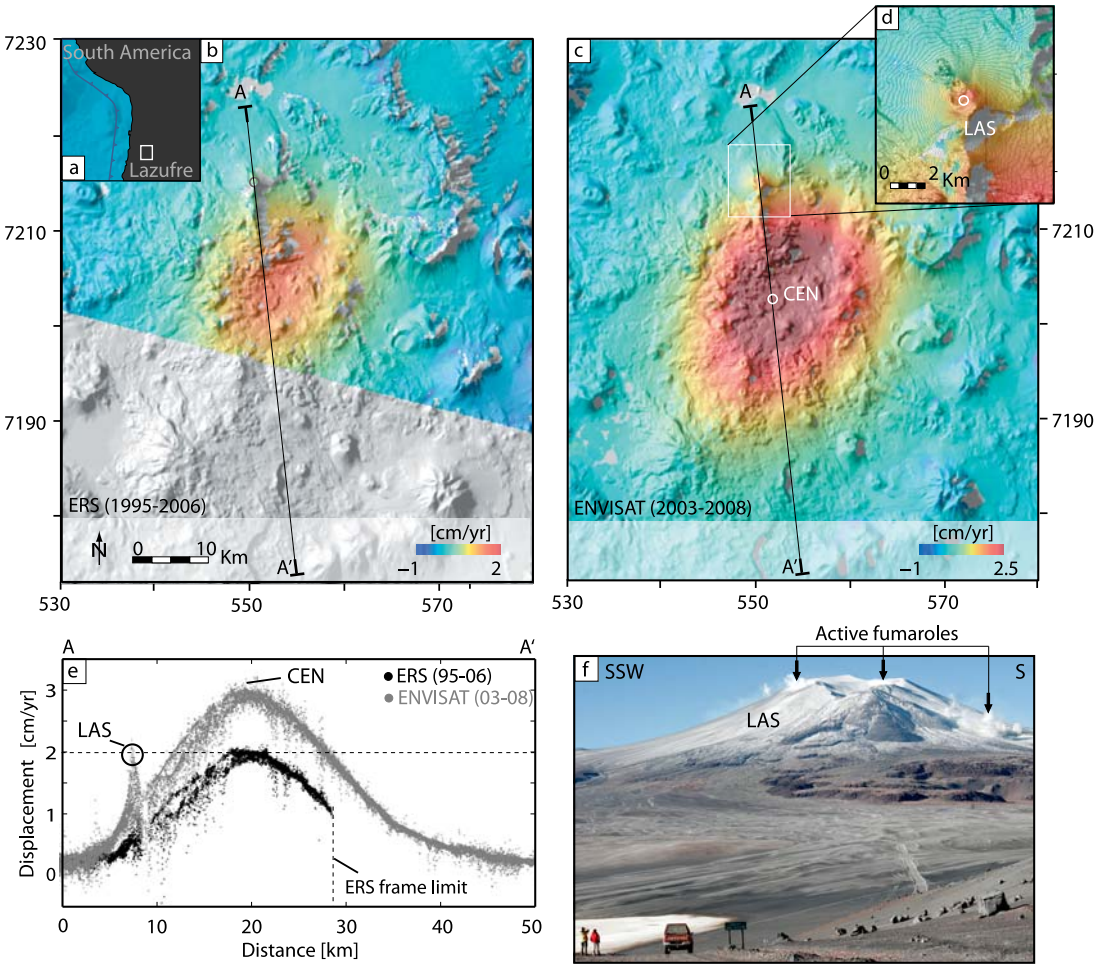

Figure 1. Deformation at the Lazufre volcanic area in the Central Andes. (a) Location of Lazufre. Shaded relief maps with InSAR observation (mean velocity map) for (b) the period from June 1995 to December 2006 (ERS) and (c) the period from April 2003 to January 2008 (ENVISAT). (d) Details of Lastarria volcano. (e) NNW-SSE profiles across the deformation areas for the ERS dataset from 1995 to 2006 (black) and for the ENVISAT dataset (grey) from 2003 to 2008. Sampling width of the cross section is 1 km. (f) Photograph of the Lastarria volcano (27th of April 2007, 9 a.m.) taken from the northwest, 10 km distant from the summit.

Because spatially the ERS and the ENVISAT acquisitions only partially overlap (Figures 1b and 1c), the SBAS analysis has been performed separately on the two datasets. Accordingly, we obtain two mean deformation velocity maps and 13-year displacement time series within the overlapping region with a standard deviations of about 0.1–0.2 cm/yr and 0.5–1 cm, respectively [*Casu et al.*, 2006].

[7] The retrieved deformation encompasses an area larger than 1800 km^2 and shows also a local deformation at the Lastarria volcano affecting an area of around 50 km^2 (Figure 1d). A NNW - SSE profile crossing the deforming area allows us to compare the deformation rate of the two datasets (Figure 1e). We found that the mean deformation rate increased from the 1995 to 2006 (ERS) period to the 2003 to 2008 (ENVISAT) period, with a rate change from 1.8 to 3.2 cm/yr (Figure 1e). The profile also shows a short-wavelength signal with lower amplitude located at Lastarria (LAS). The observed displacement rate at LAS reaches up to 2 cm/yr from 2003 to 2008, with a part of this signal being related to the large-scale deformation field.

3. Source Modeling

[8] To quantify the sources responsible for the two-scale deformations, we invert the observed signal by applying a heuristic optimization method (Simulated Annealing), which follows the approach detailed by *Kirkpatrick et al.*

Table 1. Source Parameter Results Using a Rectangular Dislocation Plane[a]

LAZUFRE	ERS 1996–2000	ENVISAT 2003–2008
Length (km)	18.7 ± 0.2	21.3 ± 0.7
Width (km)	8.5 ± 0.9	6.7 ± 2.8
Depth (km)	11.8 ± 0.2	13.3 ± 0.3
Opening (cm)	5.1 ± 0.7	41.9 ± 1.0
ΔV source (km^3)	0.008 ± 0.0016	0.059 ± 0.001

[a]*Okada* [1985]. Inversion was performed for the long wavelength signal of the Lazufre area for both ERS and ENVISAT datasets.

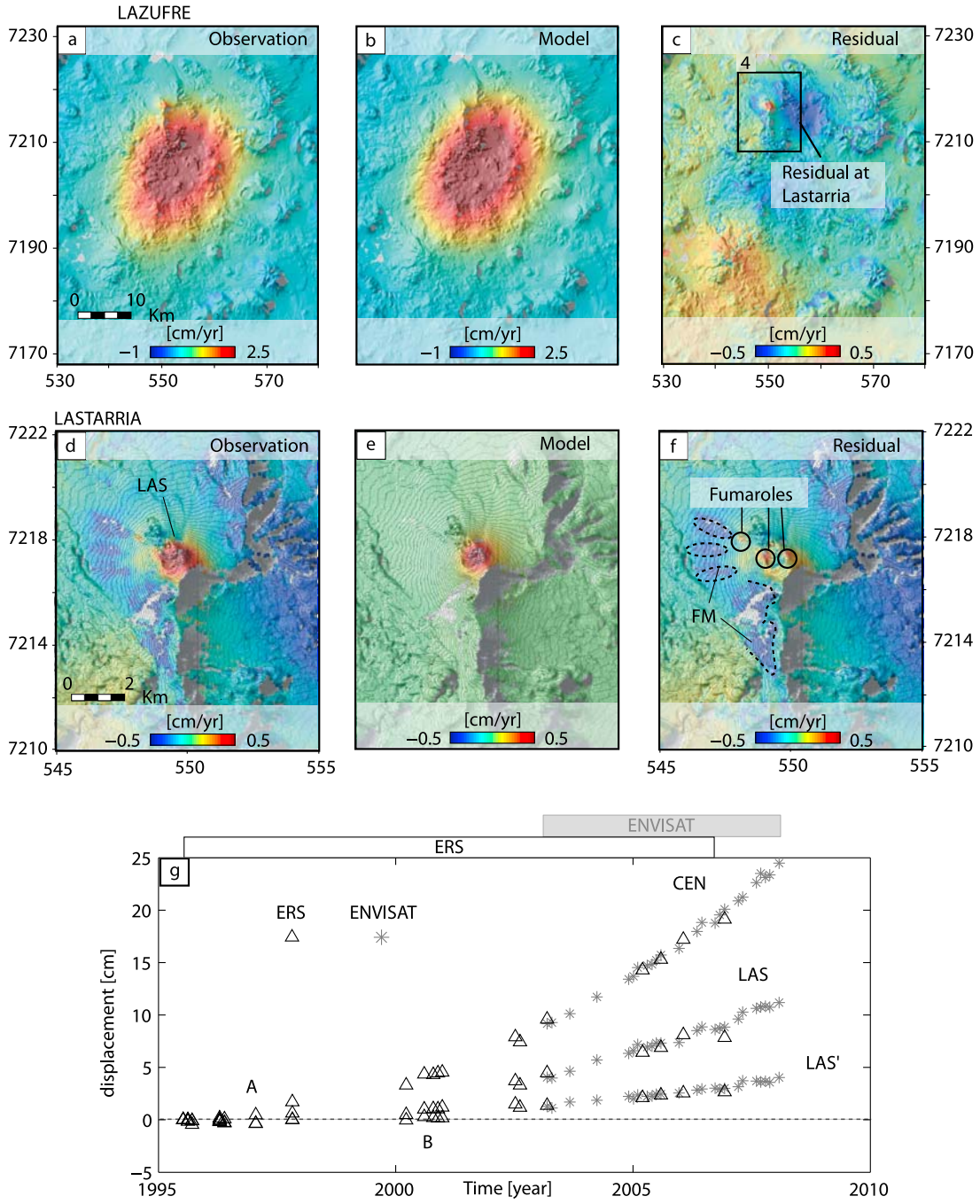

Figure 2. (a–f) Inversion results of the Lazufre deformation data for the period from 2003 to 2008 (Table 1). (a) Observation data (InSAR), (b) synthetic models, and (c) residuals. Inversion of the Lastarria signal using a finite spherical source showing (d) the observation data (InSAR), (e) the synthetic model, and (f) residuals that highlight three fumarolic areas (black circles). Dashed lines indicate flank movements (FM), which act on the western flank of the Lastarria volcano. (g) Time series plot for the ERS (black triangle) and ENVISAT (grey stars) datasets for two observations points that correspond to both maximum displacements at Lazufre (CEN) and Lastarria (LAS). LAS′ is plotted after removing the long wavelength signal to better assess the initiation of the deformation. Results may suggest a shift between both signals initiations at CEN (marked as A) and LAS′ (marked as B).

[1983]. To isolate the displacement signal we first applied the linear Pearson correlation coefficient [*Stanton*, 2001] and searched for pixels that fell within 95% of a similar trend to the maximum displacement observation point (CEN) in Figure 1. Pixels that are not affected by the deformation are thus excluded. Second, we sub-sampled the cross-correlated dataset using a regularly spaced grid (1 km) that reduces significantly the computational time without affecting the parameter estimation performance. To evaluate a confidence interval for the estimated parameters, we iterated the inversion procedure 100 times and retained the models that fall within ±5% of the minimum

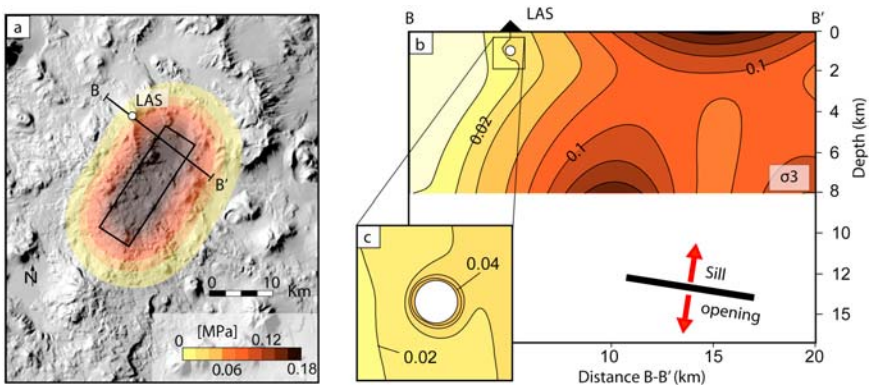

Figure 3. Stress transfer model at Lazufre for the period from 1997 to 2000. Maximum tensile stress $\sigma 3$ is caused in the area of interest by the deep source inflation (a) at the surface. The rectangle represents the best fit dislocation plane projected to the surface, (b and c) cross-section through B − B′ that shows a slight increase of the tensile stress around the simulated source of Lastarria volcano.

cost (L^2 norm), assuming as best models the mean of parameters within this range. Because the main deformation scale is very large and its source likely to be laterally extended [*Ruch et al.*, 2008], we assumed an expanded dislocation plane acting as a sill source model [*Okada*, 1985], and then estimated its parameters. Because additional geophysical and geological data are missing to elaborate more realistic models, the models were performed in an elastic half-space medium with a Poisson's ratio v = 0.25 and a Young's Modulus of E = 50 GPa. The results suggest that the source depth for both datasets is located at 12–14 km below the surface and almost constant for the entire 13-year time series (see Table 1). Residuals are generally less than 0.2 cm/yr with the exception of a near radial-symmetric deformation signal with uplift rates larger than 1 cm/yr centered on the Lastarria volcano (Figure 2a) affecting an area of about 50 km^2.

[9] We further investigated this residual deformation by applying a spherical pressurized model approximation [*McTigue*, 1987]. Because Lastarria is relatively steep-sided we also considered the topography [*Williams and Wadge*, 1998]. The residuals are again generally less than 0.2 cm/yr, with the exception of the area where the three main fumarolic fields are located, which still shows a residual signal up to 0.5 cm/yr (Figure 2a). We left the source position free, but constrained our model parameters [*Shirzaei and Walter*, 2009] to obtain pressure change values below a reasonable threshold of 10 MPa/yr, which is considered as a limit after which rock may begin to fracture [*Manga and Brodsky*, 2006]. Our best fitting models suggest a shallow spherical source, located between 0.6 and 0.9 kilometers below the Lastarria summit, in agreement with *Froger et al.* [2007]. Although the deformation at Lastarria is a short-wavelength signal, we obtained similar shallow locations using other type of source model [*Mogi*, 1958]. Therefore, because of the height of Lastarria volcano (1 km relative), the source appears to be located within the edifice. The source radius is ~0.3 km (between 230 and 360 meters) and subjected to a volume change of ~13000 m^3/yr (between 8000 and 18000 m^3/yr). The pressure change induced by the source is between 0.4 and 4 MPa/yr, cumulating in a range of 2 to 20 MPa over a five-year observation period (2003–2008). These values are compatible with the lithostatic stress values expected at such shallow depth.

4. Deformation Starts and Stress Transfer Modeling

[10] We analyzed the time evolution of the local deformation observed at Lastarria volcano after the removal of the long wavelength signal caused by the deeper source (Figure 2b, LAS and LAS′, respectively). Results may suggest a temporal delay compared with the start of the broader inflation observed at Lazufre (CEN). By assuming 1 cm accuracy to be a detection threshold, first evident deformation signal at CEN began in 1997 (marked by "A" in Figure 2b), while deformation at LAS′ (marked by "B" in Figure 2b) was uncertain before the year 2000.

[11] Numerical modeling may help to understand whether the stress field changes caused by the inflation of the deep source in the surrounding of Lastarria volcano can explain its observed activity. In our stress model calculations we quantified the change of the maximum tensile stress ($\sigma 3$), which is a common indicator for estimating occurrence and location of crack initiation [*Gudmundsson*, 2006]. Using a boundary element method [*Thomas*, 1993], we simulated the opening of the deep source by a dislocation plane for the period from 1996 to 2000 (Table 1). Because the influence of an active magmatic or hydrothermal reservoir can be approximated by a material property that is softer than the surrounding host rocks, we defined the shallow source as a void in an elastic medium [*Savin*, 1961]. Therefore, we included a spherical source at shallow depth beneath the Lastarria summit and defined a free slip boundary condition that is able to open or close, simulating passive source inflation or deflation, respectively. Deformation of this inclusion perturbs the local stress field in the surrounding region. We found that close to the shallow source, the maximum tensile stress was more than twice as large if compared to a model without such an inclusion (Figure 3). For validation, we tested the stress field change using Finite Element Method with the same initial parameters and obtain similar results. The models implied that the inflating deep source caused the maximum tensile stress at the shallow

source to increase by 0.04 MPa between 1996 and 2000, before it displayed deformation above detection threshold. Until 2008, the induced stress change cumulated at around 0.2 MPa. Although these stress changes appear to be small, comparable values are thought to have triggered volcanic elsewhere [*Manga and Brodsky*, 2006].

5. Discussion and Conclusions

[12] In the present paper, we used two InSAR datasets spanning the time interval 1995–2008 to analyze multi-scale deformation patterns in the Lazufre volcanic area and test the relationship of neighboring volcanic systems. We analyzed the deformation signals through elastic half-space models, retrieving the location and volume change of the large-scale and small-scale sources. Using stress models, we tested the hypothesis that inflation of the deeper and larger source increased the tensile stress around the shallow source and may have even triggered the local activity at Lastarria.

[13] Earthquake occurrences and volcano inflations have been proposed as triggering sources that modify the surrounding stress field and possibly reactivate dormant volcanoes. This was suggested to explain seismicity and fumarole activity at Long Valley [*Hill et al.*, 2002] or even eruptions as Karymsky and Akademia Nauk volcanoes in 1996 [*Walter*, 2007]. The amount of stress involved varies by several orders of magnitudes. Acidic dikes propagate at magmatic overpressures of up to 10 MPa, basaltic dikes at up to 1 MPa [*Jellinek and DePaolo*, 2003; *McLeod and Tait*, 1999], and may even initiate due to very small stress changes as induced by earthquakes of about 0.1 MPa or even below [*Manga and Brodsky*, 2006]. Thus, small amounts of stress change, as calculated here in the surrounding of Lastarria volcano, may induce enough perturbation to encourage unrest. A volcanic or hydrothermal source needs to be in a critical stage to be reactivated by small amount of stress change [*Hill et al.*, 2002; *Manga and Brodsky*, 2006]. Here, we estimate that 0.04 MPa accumulated until 2000 at Lastarria and increased up to 0.2 MPa until 2008. This implies that the Lastarria volcano, which is strongly affected by hydrothermal and fumarolic activity, may have been in a critical stage susceptible to very small perturbations of the surrounding stress field, while other volcanoes located in areas where the induced stress changes are higher do not show any surface deformation.

[14] Stress changes at a magmatic or hydrothermal reservoir may lead to a cascade of associated effects that are not yet fully understood. An extrinsic increase of the tensile stress around a void (magmatic or hydrothermal reservoir) might lower the pressure into it [*Savin*, 1961], generating a gradient that may in turn allow fluids or volatiles to migrate. The fluids might be trapped by the presence of a low-permeability cap that is known to partially seal active hydrothermal reservoirs at volcanoes [*Aizawa et al.*, 2009]. Comparable phenomenon was suggested to occur at other volcanic areas containing sealed hydrothermal system [*Hurwitz et al.*, 2007]. Stress changes at the reservoir walls may cause linkage of pre-existing fractures, thus leading to changes in rock permeability and encouraging fluid propagation [*Wang*, 2000]. Therefore, the observed deformation at Lastarria may be the consequence of fluid-mechanical and rock mechanical processes.

[15] The InSAR time series and stress models allow us to propose a possible relationship between two volcanic reservoirs. However, the models are simplified, assume a linear elastic material, and do not consider time dependent rheologies [*Wang*, 2000]. Material heterogeneities may affect part of the deformation signal, for instance, locally under the Lastarria volcano. Soft materials may amplify the surface deformation [*Manconi et al.*, 2007]. At Lastarria, soft material is present in the hydrothermally active regions (see Figure 1e), including the intrusive core and the fumarolic field. The effect of material heterogeneity is also locally shown by the deformation residuals at the western flank of Lastarria volcano, where the retrieved LOS displacements are negative (see Figure 2a). Our field inspection (Figure 1e) suggests that this locality matches the steep slopes >20° of the volcano and consists of unconsolidated material, implying the signal is due to localized slow-flank movements or creeping phenomena. Unless studied in further detail, however, these contributors do not allow us to construct more realistic models, which would require additional geophysical information.

[16] Therefore, our models suggest possible explanation of the processes occurring in the Lazufre volcanic area, as evidenced by the InSAR data analysis. Thus, we suggest that upward directed stress transfer occurs at Lastarria volcano, where changes of the shallow system may reflect an activity change at the deep source.

[17] **Acknowledgments.** We acknowledge discussions with Maurizio Battaglia, Valérie Cayol, José Fernández, Jean-Luc Froger and Paul Lundgren. We are grateful to Matt Pritchard for his constructive comments, and for providing us with ERS images to extend our time series analysis. Envisat data were provided by the ESA as part of CAT-1 project 3455. The research was partially funded by theDFG, grant WA1642.

References

Aizawa, K., Y. Ogawa, and T. Ishido (2009), Groundwater flow and hydrothermal systems within volcanic edifices: Delineation by electric self-potential and magnetotellurics, *J. Geophys. Res.*, *114*, B01208, doi:10.1029/2008JB005910.

Berardino, P., G. Fornaro, R. Lanari, and E. Sansosti (2002), A new algorithm for surface deformation monitoring based on small baseline differential SAR Interferograms, *IEEE Trans. Geosci. Remote Sens.*, *40*(11), 2375–2383, doi:10.1109/TGRS.2002.803792.

Casu, F., M. Manzo, and R. Lanari (2006), A quantitative assessment of the SBAS algorithm performance for surface deformation retrieval from DInSAR data, *Remote Sens. Environ.*, *102*, 195–210, doi:10.1016/j.rse.2006.01.023.

De Silva, S., and P. W. Francis (1991), *Volcanoes of the Central Andes*, 216 pp., Springer, Berlin.

Froger, J. L., D. Remy, S. Bonvalot, and D. Legrand (2007), Two scales of inflation at Lastarria-Cordon del Azufre volcanic complex, central Andes, revealed from ASAR-ENVISAT interferometric data, *Earth Planet. Sci. Lett.*, *255*(1–2), 148–163, doi:10.1016/j.epsl.2006.12.012.

Gudmundsson, A. (2006), How local stresses control magma-chamber ruptures, dyke injections, and eruptions in composite volcanoes, *Earth-Sci. Rev.*, *79*(1–2), 1–31, doi:10.1016/j.earscirev.2006.06.006.

Hill, D. P., F. Pollitz, and C. Newhall (2002), Earthquake-volcano interactions, *Phys. Today*, *55*(11), 41–47, doi:10.1063/1.1535006.

Hurwitz, S., L. B. Christiansen, and P. A. Hsieh (2007), Hydrothermal fluid flow and deformation in large calderas: Inferences from numerical simulations, *J. Geophys. Res.*, *112*, B02206, doi:10.1029/2006JB004689.

Jellinek, A. M., and D. J. DePaolo (2003), A model for the origin of large silicic magma chambers: precursors of caldera-forming eruption, *Bull. Volcanol.*, *65*, 363–381, doi:10.1007/s00445-003-0277-y.

Kirkpatrick, S., C. D. Gelatt Jr., and M. P. Vecchi (1983), Optimization by simulated annealing, *Science*, *220*(4598), 671–680, doi:10.1126/science.220.4598.671.

Manconi, A., T. R. Walter, and F. Amelung (2007), Effects of mechanical layering on volcano deformation, *Geophys. J. Int.*, *170*, 952–958, doi:10.1111/j.1365-246X.2007.03449.x.

Manga, M., and E. Brodsky (2006), Seismic triggering of eruptions in the far field: Volcanoes and geysers, *Annu. Rev. Earth Planet. Sci.*, *34*, 263–291, doi:10.1146/annurev.earth.34.031405.125125.

Massonnet, D., and K. L. Feigl (1998), Radar interferometry and its applications to changes in the Earth's surface, *Rev. Geophys.*, *36*, 441–500, doi:10.1029/97RG03139.

McLeod, P., and S. Tait (1999), The growth of dykes from magma chambers, *J. Volcanol. Geotherm. Res.*, *92*, 231–245, doi:10.1016/S0377-0273(99)00053-0.

McTigue, D. F. (1987), Elastic stress and deformation near a finite spherical magma body: Resolution of the point source paradox, *J. Geophys. Res.*, *92*, 12,931–12,940, doi:10.1029/JB092iB12p12931.

Mogi, K. (1958), Relations between the eruptions of various volcanoes and the deformations of the ground surfaces around them, *Bull. Earthquake Res. Inst. Univ. Tokyo*, *36*, 99–134.

Naranjo, J. A., and P. Francis (1987), High velocity debris avalanche at Lastarria Volcano in the north Chilean Andes, *Bull. Volcanol.*, *49*, 509–514, doi:10.1007/BF01245476.

Okada, Y. (1985), Surface deformation due to shear and tensile faults in a half-space, *Bull. Seismol. Soc. Am.*, *75*, 1135–1154.

Oncken, O., D. Hindle, J. Kley, K. Elger, P. Victor, and K. Schemmann (2006), Deformation of the central Andean upper plate system—Facts, fiction, and constraints for plateau models, in *The Andes. Active Subduction Orogeny*, *Frontiers Earth Sci.*, vol. 1, edited by O. Oncken et al., pp. 3–27, Springer, Berlin.

Pritchard, M. E., and M. Simons (2002), A satellite geodetic survey of large-scale deformation of volcanic centres in the central Andes, *Nature*, *418*(6894), 167–171, doi:10.1038/nature00872.

Pritchard, M. E., and M. Simons (2004), An InSAR-based survey of volcanic deformation in the southern Andes, *Geophys. Res. Lett.*, *31*, L15610, doi:10.1029/2004GL020545.

Ruch, J., J. Anderssohn, T. R. Walter, and M. Motagh (2008), Caldera-scale inflation of the Lazufre volcanic area, South America: Evidence from InSAR, *J. Volcanol. Geotherm. Res.*, *174*, 337–344, doi:10.1016/j.jvolgeores.2008.03.009.

Savin, G. N. (1961), *Stress Concentration Around Holes*, 430 pp., Pergamon, New York.

Shirzaei, M., and T. R. Walter (2009), Randomly iterated search and statistical competency as powerful inversion tools for deformation source modeling: Application to volcano interferometric synthetic aperture radar data, *J. Geophys. Res.*, *114*, B10401, doi:10.1029/2008JB006071.

Stanton, J. M. (2001), Galton, Pearson and the Peas: A brief history of linear regression for statistic instructors, *J. Stat. Educ.*, *9*(3), 1.

Thomas, A. L. (1993), *Poly3D: A Three-Dimensional, Polygonal Element, Displacement Discontinuity Boundary Element Computer Program With Applications to Fractures, Faults, and Cavities in the Earth's Crust*, 110 pp., Stanford Univ., Stanford, Calif.

Walter, T. R. (2007), How a tectonic earthquake may wake up volcanoes: Stress transfer during the 1996 earthquake-eruption sequence at the Karymsky Volcanic Group, Kamchatka, *Earth Planet. Sci. Lett.*, *264*, 347–359, doi:10.1016/j.epsl.2007.09.006.

Wang, H. F. (2000), *Theory of Linear Poroelasticity: With Applications to Geomechanics*, 287 pp., Princeton Univ. Press, Princeton, N. J.

Williams, C. A., and G. Wadge (1998), The effects of topography on magma chamber deformation models: Application to Mount Etna and radar interferometry, *Geophys. Res. Lett.*, *25*, 1549–1552, doi:10.1029/98GL01136.

R. Lanari, A. Manconi, A. Pepe, and G. Zeni, IREA, CNR, Via Diocleziano 328, I-80124 Napoli, Italy.

J. Ruch, M. Shirzaei, and T. R. Walter, Deutsches GeoForschungs-Zentrum, Telegrafenberg, D-14473 Potsdam, Germany. (jruch@gfz-potsdam.de)

G. Solaro, Osservatorio Vesuviano, Istituto Nazionale di Geofisica e Vulcanologia, Via Diocleziano 328, I-80124 Napoli, Italy.